

**The classical sphaleron transition rate exists and is equal to  $1.1(\alpha_w T)^4$**

*J. Ambjørn and A. Krasnitz*  
The Niels Bohr Institute  
Blegdamsvej 17, DK-2100 Copenhagen Ø, Denmark

### **Abstract**

Results of a large scale numerical simulation show that the high temperature Chern-Simons number diffusion rate in the electroweak theory has a classical limit  $\Gamma = \kappa(\alpha_w T)^4$ , where  $\kappa = 1.09 \pm 0.04$  and  $\alpha_w$  is the weak fine structure constant.

# 1 Introduction

Topology-changing transitions play an important role in the electroweak theory since they are accompanied by baryon-number violating processes [1]. At zero temperature these processes can only appear as true quantum effects since the energy of the sphaleron configuration is a barrier separating two gauge equivalent vacua [2]. At temperatures far above the sphaleron energy one would expect that this barrier height, as well as the concept of vacuum to vacuum amplitude, are irrelevant for the transition rate. Unfortunately there presently is no way to calculate analytically the transition rate at these high temperatures. From a numerical point of view the situation is not any better if we insist on a fully quantum treatment, since the only non-perturbative tool available is lattice gauge theories in the imaginary time formalism. Real time transition rates are not easily extracted in this formalism.

The object of our study is the topological charge

$$B(t) = \frac{1}{32\pi^2} \int_0^t \int d^3x F_{\mu\nu}^a \tilde{F}^{a\mu\nu} = N_{\text{cs}}(t) - N_{\text{cs}}(0), \quad (1)$$

where the Chern-Simons number

$$N_{\text{cs}}(t) \equiv \frac{1}{32\pi^2} \epsilon_{ijk} \int d^3x \left( F_{ij}^a A_k^a - \frac{1}{3} \epsilon^{abc} A_i^a A_j^b A_k^c \right). \quad (2)$$

The theory has a periodic (with period 1) potential in the  $N_{\text{cs}}$  direction. This periodicity is due to the symmetry under large gauge transformations, changing  $N_{\text{cs}}$  by an integer. There also are dynamical processes whose result for a field configuration is the same as a large gauge transformation. These processes have an integer topological charge. Due to nonlinear interactions of  $N_{\text{cs}}$  with other degrees of freedom of the theory it is expected that for large times  $t$   $B(t)$  is a random walk in a periodic  $N_{\text{cs}}$  potential

$$\langle B^2(t) \rangle_T = \Gamma V t, \quad (3)$$

where  $V$  is the space volume, by  $\langle \rangle_T$  we mean average over the canonical ensemble, and  $\Gamma$ , the diffusion constant per unit volume, is the transition rate we are interested in [4].

At high temperatures processes with an integer topological charge occur predominantly by classically allowed thermal activation rather than by quantum tunneling. Some time ago it was suggested [3] to exploit this property and to determine  $\Gamma$  entirely within the classical theory. This is done by solving *classical* equations of motion for the fields and averaging the resulting  $B^2(t)$  over the *classical* canonical ensemble. Behind this approach is the expectation that the topology-changing transitions mostly involve field fluctuations with long wavelengths and large magnitudes (hence many quanta). Such fluctuations are well described by classical statistical mechanics. An argument usually given to support this picture is as follows. Consider a classically allowed process with  $B(t) = 1$ , whereby the field configuration evolves from the vicinity of one minimum in the  $N_{\text{cs}}$  potential to the vicinity of another one. If a typical linear space-time size of the process is  $r$ , the system will cross an energy barrier of height  $E \sim 1/\alpha r$ , where  $\alpha = g^2/4\pi$ . While large  $r$  are favored energetically, at high temperatures  $r$  is unlikely to exceed the inverse of the magnetic screening mass  $m_{\text{mag}} \sim \alpha T$ . We then expect that processes with  $r \sim 1/\alpha T$  give the most important contribution to  $\Gamma$ . In the electroweak theory, where  $\alpha_w \approx 1/30$ , these  $r$  are much larger than the thermal wavelength, *i.e.*, fluctuations of size  $r$  can be treated

classically. In order to estimate the transition rate, the Boltzmann factor associated with the barrier,  $\exp(-E/T) \sim 1$ , is divided by the space-time volume  $r^4$  of the process, to give [5]

$$\Gamma = \kappa(\alpha T)^4, \quad (4)$$

where  $\kappa$  is a dimensionless constant. This estimate should be valid at temperatures far above the electroweak transition scale. We also expect that at such high temperatures the mass scales of the Higgs sector are irrelevant, and that  $\Gamma$  can be reliably obtained from a pure Yang-Mills theory.

The classical approximation offers an enormous simplification in computing real-time correlation functions. However, it is well known that classical field theory at finite temperature suffers from the Rayleigh-Jeans ultraviolet divergence. This means that, upon cutoff regularization, classical thermodynamic average of a generic observable will be sensitive to thermal fluctuations at the cutoff scale  $\Lambda$  [6]. The classical rate  $\Gamma$ , if it is to be trusted, must not show such sensitivity. This is indeed what we expect: considerations leading to the estimate (4) may be repeated for a purely classical theory which also possesses a magnetic mass  $m_{\text{mag}} \sim \alpha T$ . In the quantum case, we required separation between the magnetic and the thermal scales:  $\alpha T \ll T$ . Likewise, in the classical theory we should require separation between the magnetic and the cutoff scales:  $\alpha T \ll \Lambda$ . These two conditions make it plausible that  $\Gamma$  is not strongly affected by either quantum corrections or the classical cutoff.

On the other hand, it is not clear how the  $\Gamma$  independence of  $\Lambda$  is technically possible: after all,  $\dot{B}(t)$ , the topological charge per unit time, is an ultraviolet divergent quantity whose classical standard deviation is given perturbatively by

$$\langle (\dot{B})^2 \rangle_T = \left( \frac{1}{8\pi^2} \right)^2 \left\langle \left( \int d^3x E_i^a(x) B_i^a(A(x)) \right)^2 \right\rangle_T \sim T^2 V \Lambda^3, \quad (5)$$

where  $E_i^a$  and  $B_i^a$  are, respectively, color electric and magnetic fields, and  $V$  is the space volume. One then naturally expects the Rayleigh-Jeans divergency to show up in  $\langle B^2(t) \rangle_T$  itself.

The key point, confirmed by the numerical simulations in the following, is that the UV divergency shows up in  $\langle B^2(t) \rangle_T$  in a way that does not affect  $\Gamma$ . To see how this could be anticipated, consider the structure of  $\langle B^2(t) \rangle_T$  in some more detail. The classical motion of  $N_{\text{cs}}$  can be thought of as consisting of two pieces: “true” thermal fluctuations and a random walk between gauge equivalent vacua. If the theory did not have an infinite series of degenerate vacua,  $N_{\text{cs}}$  would simply fluctuate around zero, as it does in an Abelian theory. The properties of these thermal fluctuations can be studied perturbatively. As discussed in the Appendix, in an Abelian theory, where no random walk of  $N_{\text{cs}}$  is possible,  $\langle B^2(t) \rangle_T$  is bounded

$$\langle B^2(t) \rangle_T^{\text{Abelian}} \leq 2 \langle (N_{\text{cs}})^2 \rangle_T^{\text{Abelian}} \quad (6)$$

and at large  $t$  fluctuates around the average value

$$\nu \equiv \langle (N_{\text{cs}})^2 \rangle_T^{\text{Abelian}} \approx 0.00228 \frac{(\alpha T)^2}{a} V, \quad (7)$$

diverging, as expected, linearly with the lattice cutoff  $\Lambda = 1/a$ . In the nonabelian theory the random walk of  $N_{\text{cs}}$  is superimposed with this thermal background. A reasonable

approximation to the nonabelian  $\langle B^2(t) \rangle_T$  is then

$$\langle B^2(t) \rangle_T = c\nu + \Gamma Vt, \quad (8)$$

where  $c \approx 3$ , assuming that thermal fluctuations of  $N_{\text{cs}}$  are exactly those for three independent copies of an Abelian theory.

If we let  $\Lambda \rightarrow \infty$  for fixed  $t$  the r.h.s. of (8) diverges. On the other hand, for a fixed cutoff (8) is well approximated by (3) for large enough  $t$  and allows unambiguously to extract  $\Gamma$ . We will show that numerical simulations, using a classical thermal ensemble with a lattice cutoff  $\Lambda = 1/a$ , point to a  $\Gamma$  independent of  $a$  for sufficiently small  $a$ . On dimensional grounds this means that (4) holds classically in the continuum limit, with  $\kappa$  of (4) being a *non-perturbative constant of the classical theory*. For the gauge group  $SU(2)$  we find  $\kappa = 1.09 \pm 0.04$ . This is the central result of our work.

The ultraviolet insensitivity of  $\Gamma$  extracted from (8) might be linked to the topological aspect of the special field tensor combination  $F_{\mu\nu}^a \tilde{F}^{a\mu\nu}$  in non-abelian field theories. Replacing  $F_{\mu\nu}^a \tilde{F}^{a\mu\nu}$  by a generic bilinear of field tensors with zero average would yield a UV divergent transition rate. We illustrate this point by measuring in addition the quantity  $\eta(t)$  whose diffusion rate is related to the shear viscosity of the gluon plasma [14]:

$$\eta(t) = \int_0^t dt \int d^3x (T_{11} - T_{22}), \quad (9)$$

where  $T_{ij}$  are components of the energy-momentum tensor.

## 2 The model and the numerical method

The philosophy behind the classical measurements of real-time quantities has been presented in detail in a number of articles [7, 8]. Here we only concentrate on the essential technical points. We work in the temporal gauge. The classical dynamics of  $SU(2)$  Yang-Mills theory on the lattice is given by Kogut-Susskind Hamiltonian

$$H = \frac{1}{2} \sum_l E_l^\alpha E_l^\alpha + \sum_{\square} \left( 1 - \frac{1}{2} \text{Tr} U_{\square} \right). \quad (10)$$

The variable set consists of  $SU(2)$  matrices  $U_l$  and lattice analogs of electric field  $E_l$ , both residing on the links of a cubic lattice. We shall also use notation  $l = j, n$  for a link emanating from site  $j$  in positive direction  $n$ . The second term in (10) is the standard plaquette term, representing the color magnetic energy. Every variable  $v$  evolves in time according to its canonical equation  $\dot{v} = \{H, v\}$ , derived using Poisson brackets between the independent variables:

$$\{E_l^\alpha, E_{l'}^\beta\} = 2\delta_{ll'} \epsilon^{\alpha\beta\gamma} E_l^\gamma; \quad \{E_l^\alpha, U_{l'}\} = -i\delta_{ll'} U_l \sigma^\alpha; \quad \{U_l, U_{l'}\} = 0 \quad (11)$$

(no summation over repeated  $l$ ;  $\sigma^\alpha$  are the Pauli matrices). The time evolution is subject to the set of three Gauss' constraints per site

$$\sum_n \left( \overline{E}_{j,n}^\alpha - E_{j-n,n}^\alpha \right) = 0, \quad (12)$$

where

$$\overline{E}_{j,n}^\alpha \equiv \frac{1}{2} E_{j,n}^\beta \text{Tr} \left( \sigma^\alpha U_{j,n} \sigma^\beta U_{j,n}^\dagger \right).$$

These constraints are to be imposed on initial conditions. We use the leapfrog algorithm to integrate the equations of motion, performing *exact* integration of the  $E$  equations for fixed  $U$  and of the  $U$  equations for fixed  $E$ . In this way the Gauss' laws are obeyed exactly, independently of the time step, and the only source of spurious static charge is the limited computer accuracy.

The increment of Chern-Simons number is computed as in (1) with the topological charge per unit time approximated by

$$\dot{N}_{\text{cs}} = \frac{i}{32\pi^2} \sum_{j,n} \left( \overline{E}_{j,n}^\alpha + E_{j-n,n}^\alpha \right) \sum_{\square_{j,n}} \text{Tr} \left( U_{\square_{j,n}} \sigma^\alpha \right), \quad (13)$$

where  $\square_{j,n}$  denotes plaquettes in the plane perpendicular to direction  $n$ , running counter-clockwise in that plane, and beginning and ending at site  $j$ .

Our purpose is to study the average of  $B^2(t)$  (*cf* (1)) over the thermal ensemble of initial field configurations. Due to the presence of first-class constraints (Gauss' laws) this point is nontrivial. The initial configurations must satisfy the constraints and be thermally distributed in the reduced phase space of physical, gauge-invariant degrees of freedom. This goal is achieved by using the constraint-respecting Langevin algorithm. The set of Langevin equations reads ( $\beta$  is the inverse temperature in lattice units)

$$\dot{U}_{j,k} = \{H, U_{j,k}\} + (\Gamma_{j,mn}(t) - \beta\{T_{j,mn}, H\}) \{T_{j,mn}, U_{j,k}\}; \quad \dot{E}_l^\alpha = \{H, E_l^\alpha\}, \quad (14)$$

where, for fixed  $j$ ,  $T_{j,mn} \equiv \sqrt{\gamma} \overline{E}_{j,m}^\alpha \overline{E}_{j,n}^\alpha$  (assuming for definiteness  $m \leq n$ ), and  $\Gamma_{j,mn}(t)$  is a random variable with zero average and correlation

$$\langle \Gamma_{j,mn}(t) \Gamma_{j',m'n'}(t') \rangle = 2\delta(t-t') \delta_{jj'} \delta_{mn,m'n'}.$$

We are free to choose the friction coefficient  $\gamma > 0$ . This freedom can be used to optimize the algorithm performance. Evolution generated by (14) is not to be confused with real-time evolution according to canonical equations of motion: the sole purpose of (14) is to bring the system in question to thermal equilibrium at temperature  $1/\beta$ . The set of equations (14) is integrated numerically using a modified leapfrog algorithm, which obeys the Gauss' laws as accurately as a computer arithmetic allows. For a more detailed description of the algorithm we refer to [9].

Results of simulation must eventually be converted from lattice units to the physical ones in the continuum. To do so it is convenient to parametrize the link matrices as  $U_l = \exp(ia\sigma^\alpha A_l^\alpha/2)$  where  $a$  is the lattice spacing and  $A_l^\alpha$  is the gauge potential. It follows from the equation of motion for  $U_l$  that  $E_l^\alpha = i\text{Tr}(\sigma^\alpha U_l^\dagger \dot{U}_l)/2$ . Therefore for small  $a$  (10) takes form

$$H \approx \frac{a^2}{8} \sum_{j,n} \left( \dot{A}_{j,n}^\alpha \dot{A}_{j,n}^\alpha + a^2 B_{j,n}^\alpha B_{j,n}^\alpha \right), \quad (15)$$

where  $B_{j,n}^\alpha$  is a chromo-magnetic field. Comparing (15) to the standard continuum Hamiltonian

$$H_C = \frac{1}{2g^2} \int d^3x \left( \dot{A}_i^\alpha \dot{A}_i^\alpha + B_i^\alpha B_i^\alpha \right)$$

we find the correspondence between the time and the temperature expressed in lattice ( $L$ ) and continuum ( $C$ ) units:

$$t_C = at_L; \quad T_C = \frac{4}{g^2 a} T_L. \quad (16)$$

Taking into account that  $N_{\text{cs}}$  itself is a dimensionless quantity, (4) on the lattice takes form  $\Gamma_L = \kappa(T_L/\pi)^4$ , where the lattice rate  $\Gamma_L$  is per unit cell.

### 3 Results

We performed series of simulations using methods described in the previous section for three values of the inverse lattice temperature  $\beta = 10, 12, 14$  on lattices of equal size  $L_L$  and periodic boundary conditions in all spatial directions. The value of  $L_L$  ranged between 8 and 32. Between 20 and 60 statistically independent initial configurations were produced for every  $\beta, L_L$  pair (60 for the largest volumes, used for the estimate of  $\kappa$ ). At low temperatures considered the system is only weakly nonlinear, and we expect an average energy per physical degree of freedom to be close to  $1/2\beta$ . This is indeed what we observe: the average chromo-electric energy per site was found to be  $3/\beta$  with a three-digit accuracy. Our measurement results for the topological charge density are also close to the perturbative estimate (23).

Every independent initial configuration was let evolve in real time for 5000 time units. We used the integration time step of 0.05 for the classical equations of motion. From our experience in earlier work [7] we know that reducing the time step beyond this value has negligible impact on the diffusion of Chern-Simons number. During the real-time evolution the value of  $B(t)$ , determined by numerically integrating the lattice topological charge per unit time, was recorded with intervals between 0.5 and 1 time unit. In the same way, we recorded the time history of  $\eta(t)$ . Thus our results for  $\langle B^2(t) \rangle_T$ , discussed in the following, represent averaging both over the canonical ensemble of initial configurations and within every individual real-time trajectory. The same averaging method was used in earlier work on a low-dimensional model [8].

A typical plot of  $\langle B^2(t) \rangle_T$  as a function of the lag  $t$  is shown in Figures 1 and 2. As expected, for very short lags ( $t \leq 1$ )  $\langle B^2(t) \rangle_T$  is mostly accounted for by the perturbative result obtained from (22). For larger lags a random walk of  $N_{cs}$  sets in, and  $\langle B^2(t) \rangle_T$  rapidly approaches a linear asymptote. Thus, for large enough  $t$ ,  $\langle B^2(t) \rangle_T$  can be fitted to the form (8). The range of  $t$  suitable for this linear fit is bounded from below by the initial transient behavior, and from above by the growing statistical errors in our determination of  $\langle B^2(t) \rangle_T$ . With the temperatures and lattice sizes used, we found the optimal range to be approximately  $40 < t < 200$ . As Figures 1 and 2 indicate, at these lags  $\langle B^2(t) \rangle_T$  is dominated by the nonperturbative effects. The central values of  $\langle B^2(t) \rangle_T$  for larger  $t$  are consistent with linear dependence on  $t$ .

We determined the coefficient  $\kappa$  of (4) by performing a correlated fit of  $\langle B^2(t) \rangle_T$  to the form (8) for data points within the optimal range. As Figure 3 shows, the values of  $\kappa$  for different combinations of  $\beta$  and  $L_L$  depend, to a good approximation, on a dimensionless ratio  $L_L/\beta$  (note, in particular, the equality of  $\kappa$  values for  $\beta = 12, L_L = 12$  and for  $\beta = 14, L_L = 14$ ). We conclude that in the range of temperatures considered  $\kappa$  is nearly insensitive to the lattice spacing, *i.e.*, close to a finite continuum limit. On the other hand,  $\kappa$  exhibits strong finite-size effects and grows rapidly for  $L_L/\beta \leq 2$ . This is in agreement with our expectation that the diffusion of  $N_{cs}$  is dominated by large-scale structures whose linear size is of order  $\beta$ . Once the lattice is too small to accommodate objects of this size, the rate rapidly decreases<sup>1</sup>. For large  $L_L/\beta > 2$   $\kappa$  reaches a constant value. In fact, the length scale at which  $\kappa$  saturates can be naturally interpreted in terms of magnetic mass,  $m_m = 0.466g^2T$  in physical units [11]:  $\kappa$  stops growing as soon as the lattice size

<sup>1</sup>That the sphaleron-like transitions are related to large scale objects has been verified directly by “freezing” the time evolution in the neighborhood of  $N_{cs} = n + 1/2$ . One finds energy profiles corresponding to extended object [10], in contrast to the situation when one is far from  $N_{cs} = n + 1/2$ . In addition one could check that level crossing occurred as expected from continuum physics.

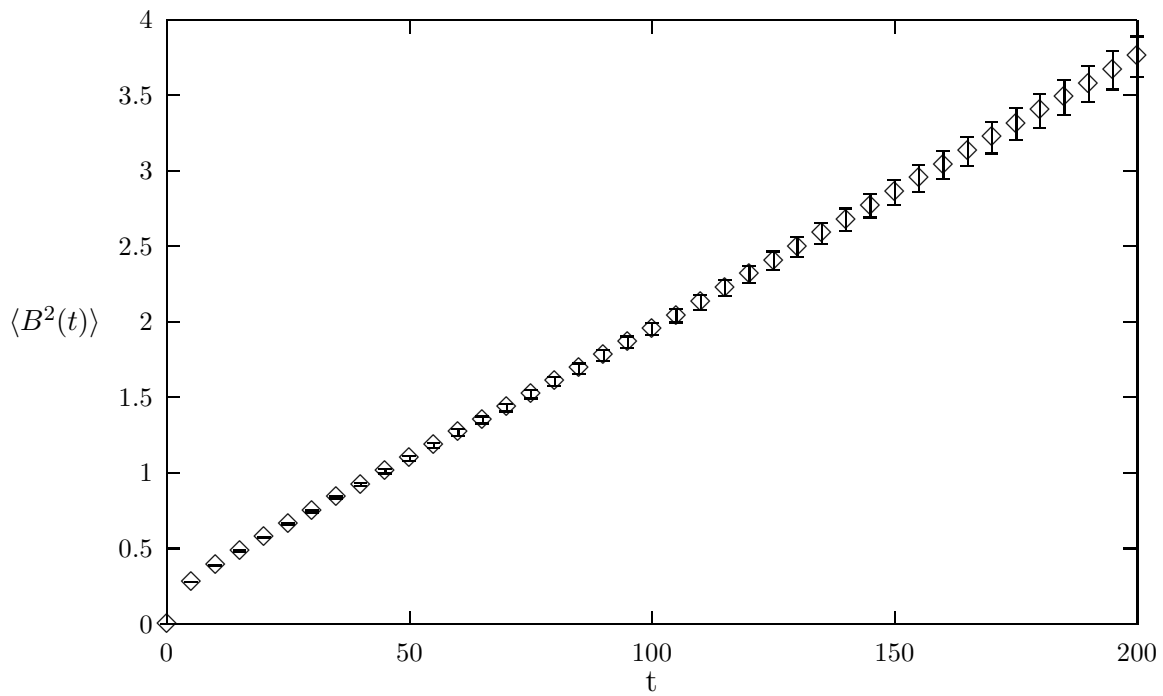


Figure 1: Diffusion of  $N_{cs}$ : mean square of  $B(t)$  as a function of the lag  $t$  for  $\beta = 12$ ,  $L_L = 32$ .

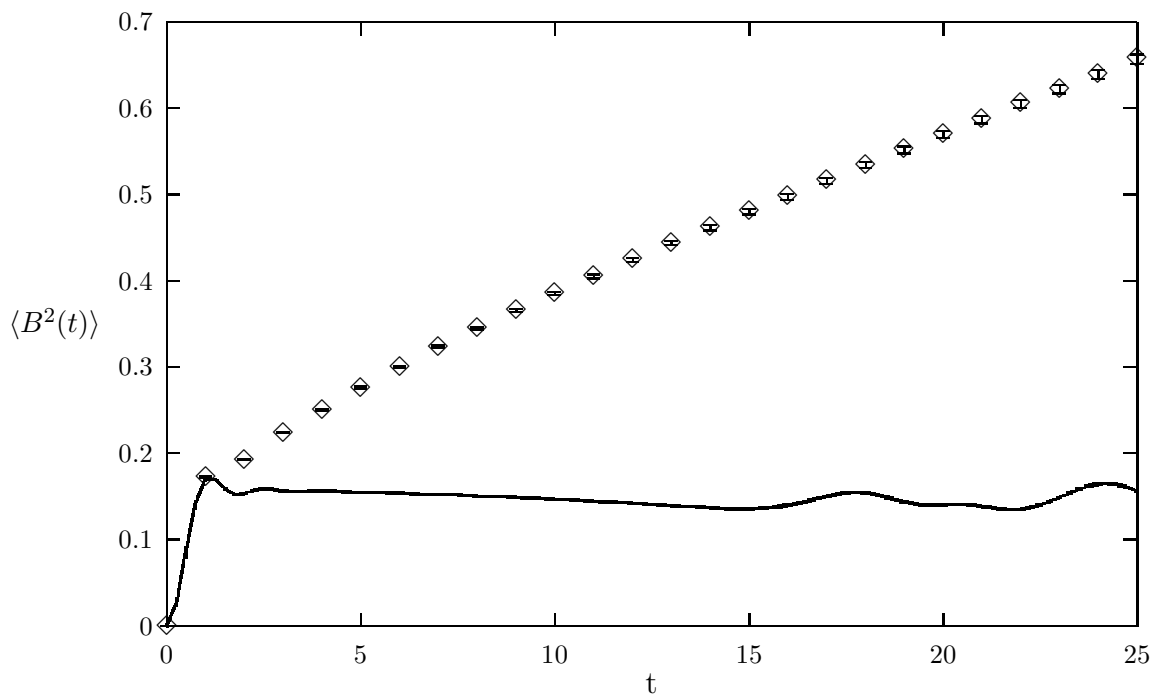


Figure 2: An enhanced region of  $0 \leq t \leq 25$  of Figure 1. The perturbative estimate of  $\langle B^2(t) \rangle_T$  is shown by the solid curve.

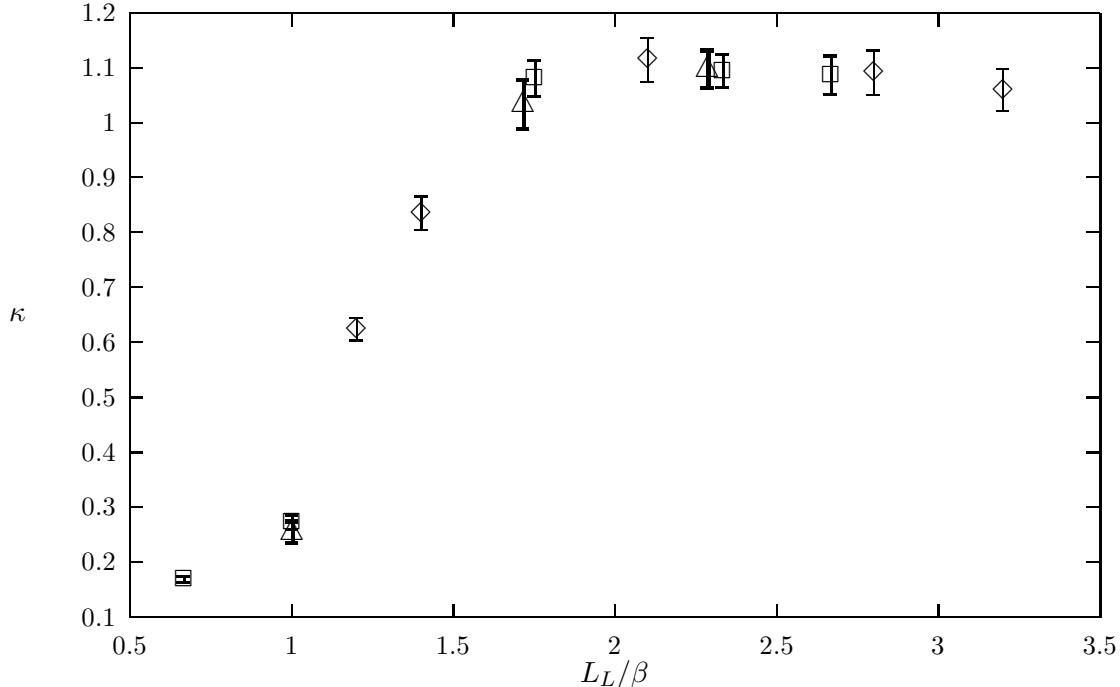


Figure 3: The rate prefactor  $\kappa$  dependence on the dimensionless parameter  $L_L/\beta$ . The data points are for  $\beta = 10$  (diamonds), 12 (squares), and 14 (triangles).

exceeds twice the inverse magnetic mass (the factor of 2 relating the two lengths is to be expected with periodic boundary conditions). Our estimate, based on  $\beta = 12, L_L = 32$  is  $\kappa = 1.09 \pm 0.04$ . Estimates from other large-volume measurements are consistent with this one within the error bars.

Our results for  $\kappa$  are in sharp contrast with those for the shear viscosity, extracted from the diffusion rate of  $\eta(t)$ . In the chosen range of temperatures  $\eta(t)$  behaves as an underdamped random walk, and determination of the corresponding diffusion constant requires knowledge of  $\langle \eta^2(t) \rangle_T$  at lags  $t$  of the order of 1000 (as compared to  $t \leq 200$  for the Chern-Simons number), making it a difficult task. As Figure 4 shows, the corresponding diffusion rate  $\Gamma_\eta$  shows no marked temperature or finite-size dependence. The absence of finite size effects for  $\Gamma_\eta$  indicates that, unlike  $\kappa$ , this quantity is not predominantly sensitive to long-wavelength modes of the system. Independence of  $\Gamma_\eta$  of the temperature means, on dimensional grounds, that  $\Gamma_\eta$ , and hence the classical shear viscosity, diverges as  $a^{-4}$ , where  $a$  is the lattice spacing. This cutoff dependence of transport coefficients is found in a similar situation in condensed-matter physics, for phonons at temperatures far above the Debye temperature [15].

## 4 Discussion

We have seen that  $\kappa \approx 1$  in a classical  $SU(2)$  gauge theory, and that we consequently have an observable (the diffusion rate between gauge equivalent non-Abelian vacua) which is not plagued by the generic ultraviolet thermal fluctuations of classical field theory. In addition we expect that the result obtained describes the high temperature limit of the classical field theory corresponding to the standard model.



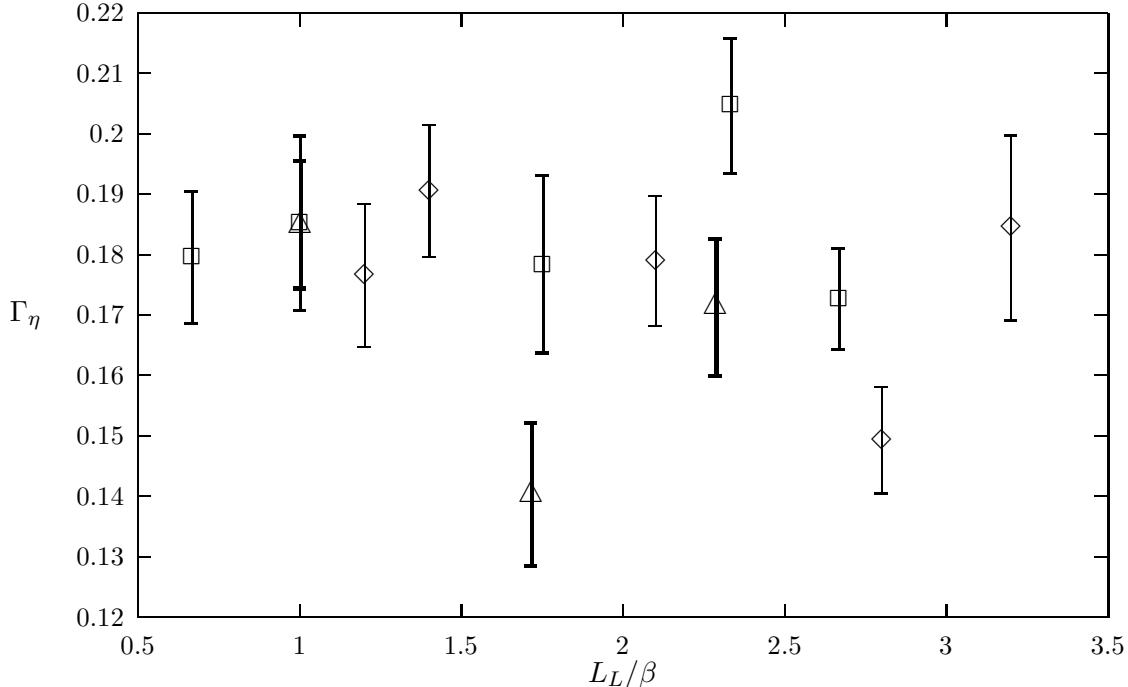


Figure 4: Diffusion constant per unit volume  $\Gamma_\eta$  of  $\eta(t)$  plotted against the dimensionless parameter  $L_L/\beta$ . The data points are for  $\beta = 10$  (diamonds), 12 (squares), and 14 (triangles).

While this result is interesting by itself, it is of even more interest to understand to what extent it is a good approximation to the full quantum theory. In the Introduction we gave qualitative arguments in favor of reasonable agreement between the classical result for the rate and the full quantum one, essentially reproducing the considerations which originally led Grigoriev, Rubakov and Shaposhnikov to suggest the classical real time method. Unfortunately, not much is known at present about the size and functional form of quantum corrections to dynamical, real-time quantities. The best we can offer is an educated guess based on a much better understood relation between the static properties of the quantum theory and of the effective dimensionally reduced one [12, 13]. The full thermal path integral, where the bosonic fields obey periodic boundary conditions in the imaginary time direction, reduces in the high temperature limit to a partition function of a three-dimensional statistical mechanical problem. This partition function inherits the  $UV$  thermal cutoff from the underlying quantum field theory. If a lattice regularization is used in the quantum theory, the spatial part of this lattice will provide the regularization of the thermal three-dimensional theory. It is known that dimensional reduction is not completely equivalent to the classical approximation. The correspondence between the two is conveniently described in terms of the field component  $A_0(x)$  which is the Lagrange multiplier of the Gauss' law. The latter may be imposed with the help of a  $\delta$ -function factor in the classical statistical weight. Alternatively, one can introduce  $A_0(x)$  and integrate out the color electric fields. The classical partition function then takes form

$$Z = \int \mathcal{D}A_i \mathcal{D}A_0 e^{-S_{\text{eff}}(A_i, A_0)}, \quad (17)$$

where

$$S_{\text{eff}}(A) = \frac{1}{4g^2T} \int d^3x \left[ F_{ij}^a F_{ij}^a + (D_i^{ab} A_0^b)^2 \right]. \quad (18)$$

On the other hand, the dimensionally reduced partition function has the same form as (17), but this time the effective action includes Higgs potential terms for  $A_0$  and reads

$$S_{\text{eff}}(A) = \frac{1}{4g^2(T)T} \int d^3x \left[ F_{ij}^a F_{ij}^a + (D_i^{ab} A_0^b)^2 + \mu(T)(A_0^a)^2 + cg(T)^2((A_0^a)^2)^2 + \dots \right], \quad (19)$$

where the parameters  $g(T)$  and  $\mu(T)$  are calculable functions of the temperature,  $g(T)$  being the running, temperature dependent coupling constant, unlike in the purely classical case. The important point is that, despite the apparent inequivalence of the two partition functions, we do not expect any qualitative difference between the dimensionally reduced theory given by (19) and the classical one given by (18), since they both are in the confined phase. In particular, both theories should give a magnetic screening mass of order  $g^2T$ . It therefore seems likely that the classical theory is able to generate the approximately correct non-perturbative behavior at the magnetic-mass scale, and that the replacement  $\alpha_w \rightarrow \alpha_w(T)$  in the classical expression (4) yields a reasonable transition rate estimate in the full theory.

## Acknowledgments

We thank L. McLerran and M.E. Shaposhnikov for useful comments. This work was supported by the Danish Research Council under contract No. 9500713. The bulk of the simulations was performed on the Cray-C92 and the SP2 supercomputers at UNI-C.

## Appendix

In this Appendix we briefly describe thermal properties of Chern-Simons number in the noncompact classical U(1) theory whose lattice Hamiltonian is

$$H \equiv \frac{1}{2} \sum_{j,n} E_{j,n}^2 + \frac{1}{4} \sum_{j,m \neq n} (\theta_{j,n} + \theta_{j+n,m} - \theta_{j+m,n} - \theta_{j,m})^2, \quad (20)$$

where, in the usual lattice notation,  $j$  are sites and  $m, n$  are positive directions on a cubic lattice, and  $\theta$  are lattice gauge potentials, whose conjugate momenta  $E_{j,n}$  are the electric fields. Note that upon substitution  $U_{j,n} = \exp(i\sigma^\alpha \theta_{j,n}^\alpha)$  and linearization (10) reduces to (20) summed over color indices  $\alpha$ . Imposing the Coulomb gauge

$$\sum_n (\theta_{j,n} - \theta_{j-n,n}) = 0,$$

we eliminate longitudinal degrees of freedom (the electric field is transversal by the Gauss' law). In momentum representation (20) becomes

$$H = \frac{1}{2} \sum_p \left[ \mathcal{E}_p^i \mathcal{E}_{-p}^i + 4 \sum_m \sin^2 \left( \frac{p_m}{2} \right) a_p^i a_{-p}^i \right],$$

where the Cartesian components of the momentum are  $p_m = 2\pi l_m / L_L$  with integer  $1 - L_L/2 \leq l_m \leq L_L/2$  on an  $L_L^3$  lattice with periodic boundary conditions,  $a_{-p}^i = (a_p^i)^*$  is a

photon field with momentum  $p$  and polarization  $i$ , and  $\mathcal{E}_p^i = (\mathcal{E}_{-p}^i)^*$  are electric fields in momentum space. It is easy to see that a mode with momentum  $p$  has an eigenfrequency

$$\omega_p = 2\sqrt{\sum_m \sin^2\left(\frac{p_m}{2}\right)}.$$

In the same notation the Chern-Simons number is

$$\begin{aligned} N_{\text{cs}} &= \frac{1}{32\pi^2} \epsilon_{lmn} \sum_j (\theta_{j-n,n} + \theta_{j,n}) (\theta_{j-l+m,l} + \theta_{j+m,l} - \theta_{j-m,l} - \theta_{j-l-m,l}) \\ &= \frac{1}{4\pi^2 i} \epsilon_{lmn} \sum_p e^{i(p_l - p_n)/2} \cos\left(\frac{p_l}{2}\right) \cos\left(\frac{p_n}{2}\right) \sin(p_m) e^i(p)_n e^j(-p)_l a_p^i a_{-p}^j, \end{aligned} \quad (21)$$

where the transverse polarization vectors  $e^i(p)$  on the lattice have the properties

$$e^i(-p) = (e^i(p))^*; \quad e^i(p)_n e^j(-p)_n = \delta^{ij}; \quad e^i(p)_l e^i(-p)_n = \delta_{ln} - e^{\frac{i}{2}(p_l - p_n)} \frac{\sin\left(\frac{p_l}{2}\right) \sin\left(\frac{p_n}{2}\right)}{\sum_r \sin^2\left(\frac{p_r}{2}\right)}.$$

Using these properties, and performing a straightforward Gaussian integration with the thermal weight  $\exp(-\beta H)$ , one obtains the autocorrelation function

$$\langle N_{\text{cs}}(t) N_{\text{cs}}(0) \rangle_T = \frac{1}{4\pi^4 \beta^2} \sum_p \frac{\cos^2(\omega_p t)}{\omega_p^2} \prod_l \cos^2\left(\frac{p_l}{2}\right). \quad (22)$$

This expression can be explicitly evaluated for any finite lattice. The thermal width  $\nu$  of Abelian  $N_{\text{cs}}$  is given by (22) at  $t = 0$ . In the limit  $L_L \rightarrow \infty$  the sum in (22) may be replaced by an integral, and  $\nu$  becomes an extensive quantity:  $\nu \approx 6.930 \times 10^{-4} \beta^{-2} L_L^3$ . We used this estimate, together with the conversion rule (16), to obtain (7). Note that the long-time behavior of (22) depends on the order in which the thermodynamic  $L_L \rightarrow \infty$  and the  $t \rightarrow \infty$  limits are taken: if the latter is taken first (which is the case of practical interest here) on a finite-size lattice, (22) will at long times fluctuate around  $\nu$  and not approach zero, as can be verified by taking time average of (22) over a long time interval.

Another useful Abelian quantity is the thermal width of  $\partial_t N_{\text{cs}}$ . Taking time derivative of (21) and averaging over the thermal ensemble yields

$$\langle \dot{N}_{\text{cs}}^2 \rangle_T = \frac{1}{2\pi^4 \beta^2} \sum_p \prod_l \cos^2\left(\frac{p_l}{2}\right) \rightarrow \frac{L_L^3}{16\pi^4 \beta^2}, \quad (23)$$

where in the last step the large-volume limit was taken.

## References

- [1] G. 't Hooft, Phys.Rev.Lett. 37 (1976) 8; Phys.Rev D14 (1976) 3432.
- [2] F. Klinkhamer and N. Manton, Phys.Rev. D30 (1984) 2212.
- [3] D. Yu. Grigoriev and V.A. Rubakov, Nucl.Phys. B299, (1988) 671.  
D. Yu. Grigoriev, V.A. Rubakov and M.E. Shaposhnikov, Nucl.Phys. B326 (1989) 737; Phys.Lett. B216 (1989) 172.
- [4] S.Yu. Khlebnikov and M.E. Shaposhnikov, Nucl.Phys. B308 (1988) 885.

- [5] P. Arnold and L. McLerran, Phys.Rev D36 (1987) 581.
- [6] D. Bödeker, L. McLerran and A. Smilga, *Really Computing Non-perturbative Real Time Correlation Functions*, hep-th/9504123.
- [7] J. Ambjørn, T. Askgaard, H. Porter and M. Shaposhnikov, Nucl.Phys.B353 (1991) 346; Phys.Lett. B244 (1990) 479.
- [8] P. de Forcrand, A. Krasnitz, and R. Potting, Phys.Rev. D50 (1994) R6054.
- [9] A. Krasnitz, *Thermalization algorithms for classical gauge theories*, NBI report NBI-HE-95-25, hep-lat/9507025, to be published in Nucl.Phys. B; Nucl.Phys. B (Proc. Suppl.) 42 (1995) 885.
- [10] J. Ambjørn and K. Farakos, Phys.Lett.B294 (1992) 248.  
J. Ambjørn, K. Farakos, S. Hands, G. Koutsoumbas and G. Thorleifsson, Nucl.Phys. B425 (1994) 39.
- [11] U.M. Heller, F. Karsch, and J. Rank, *The gluon propagator at high temperature*, Bielefeld report BI-TP 95/21, hep-lat/9505016.
- [12] T. Reisz, Z.f.Phys. C53 (1992) 169.  
P. Lacock, D.E. Miller and T. Reisz, Nucl.Phys. B369 (1992) 501.  
L. Kärkkäinen, P. Lacock, B. Petersson, D.E. Miller and T. Reisz, Nucl.Phys. B395 (1993) 733.
- [13] K. Farakos, K. Kajantie, K. Rummukainen and M.E. Shaposhnikov, Nucl.Phys. B425 (1994) 67; Nucl.Phys.B442 (1995) 317; Phys.Lett.B336 (1994) 494.
- [14] F. Karsch and H.W. Wyld, Phys.Rev. D35 (1987) 2518.
- [15] R. Berman, *Thermal conduction in solids*, Clarendon Press, Oxford (1976) 14.